

XU Zhu-an, SHEN Jing-qin, ZHU Zeng-wei

The vortex-like excitations detected by Nernst signals in high- T_c superconductors

© Higher Education Press and Springer-Verlag 2006

Abstract The nature of the pseudogap state and its relation to the d-wave superconductivity in high- T_c superconductors is still an open issue. The vortex-like excitations detected by the Nernst effect measurements exist in a certain temperature range above superconducting transition temperature T_c , which strongly support that the pseudogap phase is characterized by finite pairing amplitude with strong phase fluctuations and imply that the phase transition at T_c is driven by the loss of long-range phase coherence. We first briefly introduce the electronic phase diagram and pseudogap state of high- T_c superconductors, and then review the results of Nernst effect for different high- T_c superconductors. Related theoretical models are also discussed.

Keywords high- T_c superconductors, pseudogap, vortex-like excitations, phase fluctuations, Nernst effect

PACS numbers 74.40+k, 72.15.Jf, 74.72.-h, 74.25.Fy

1 Introduction

The mechanism of high- T_c superconductivity in cuprates has been one of the most puzzling problems in condensed matter physics since their discovery in 1986. Not only their superconducting properties are in contrast to those of conventional BCS-type superconductors, but also their normal-state properties deviate severely from the predictions of Fermi liquid theory. The energy gap (called superconducting gap) is one of the defining properties of a superconductor.

Experimental probes like the frequency-dependent con-

ductivity [1], the angle-resolved photoemission spectra (ARPES) [2], the Raman scattering spectra [3], and the tunneling conductance [4] have found that the energy gap in the cuprates does not show similar behavior as in a conventional superconductor. The depression of excitations is incomplete and often starts well above T_c in the normal state. Now this behavior is ascribed to the d-wave nature of the superconducting order parameter and the persistence of a pseudogap (PG) in the normal state [5]. The term “pseudogap” means that such a gap is an incomplete gap. That is, some regions of Fermi surface (FS) become gapped, and some other regions retain their conducting properties.

The opening of PG has significant effect on both the in-plane and c -axis transport properties [6]. It is well known that the variation of in-plane resistivity is linear with temperature for a large temperature range extending from 10–1 000 K in optimally doped high- T_c superconductors (HTS) [7]. In the underdoped HTS, the presence of the pseudogap causes striking deviations from the linear behavior. Bucher *et al.* observe a reduced in-plane resistivity in $\text{YBa}_2\text{Cu}_4\text{O}_8$ (Y124) below T^* where the pseudogap opening is seen by NMR [8]. Complete studies of the doping dependence of the characteristic temperature T^* determined by the transport measurements have been done for $\text{La}_{2-x}\text{Sr}_x\text{CuO}_4$ (LSCO) [9], $\text{YBa}_2\text{Cu}_3\text{O}_{6+x}$ (YBCO) [10], and $\text{Bi}_2\text{Sr}_2\text{CaCu}_2\text{O}_{8+\delta}$ (Bi-2212) [11]. All the studies reach a consensus that T^* decreases monotonously with increasing doping level (p). The inverse of Hall coefficient (R_H^{-1}) is also linear with temperature above the pseudogap temperature T^* , whereas the cotangent of Hall angle $\cot \theta$ displays a T^2 temperature dependence [12]. However, the characteristic temperature where $\cot \theta$ deviates from the T^2 temperature dependence, found to lie between T_c and T^* , defines another crossover line in the temperature versus doping (p) phase diagram [13]. Actually, the Knight shift and the spin-lattice relaxation time in the Cu^{63} NMR measurement [8] also define two different characteristic temperatures.

XU Zhu-an (✉), SHEN Jing-qin, ZHU Zeng-wei
Department of Physics, Zhejiang University, Hangzhou 310027, China
E-mail: zhuan@zju.edu.cn

Received April 10, 2006

So some questions regarding the nature of pseudogap are raised now. What is the relationship between superconducting gap and pseudogap? What is the origin of pseudogap and Cooper pairs? Where the T^* line will terminate in the overdoped region? An explanation of the pseudogap phenomenon is regarded as one of the most important unresolved questions in the theory of superconductivity. Due to the extremely complex structural and electronic nature of the cuprates, and the somewhat controversial nature of much of the current experimental data, there are many theoretical attempts to explain pseudogap behavior. In general, the theoretic models can be divided into three categories according to the relationship between the pseudogap state and superconducting state in these models: (1) The pseudogap state is regarded as a precursor to superconductivity. Emery and Kivelson (EK model) [14] have developed a preformed pair model of the pseudogap in which incoherent Cooper pairs form below T^* and phase order or Bose condensation of Cooper pairs establish superconductivity at T_c . These models predict that T^* line should merge with T_c line gradually in the overdoped regime. (2) In the Anderson's spin-charge separation scenario [15–16], the spinons become paired to form a gap at T^* in the spin excitations, identified as the pseudogap. Then, the holons Bose-condense at T_c to form the superconducting state. (3) In some other theoretic models, the pseudogap is induced by a kind of fluctuation of other orders (such as antiferromagnetic fluctuations, spin waves, charge-density waves, or stripes) which competes or coexists with superconductivity. A quantum critical point (QCP) in the overdoped regime is predicted by the theoretic models [17–18] in this category and the T^* line should drop to zero temperature around QCP. It requires experimental investigations to testify whether there is any QCP near the $x \sim 0.19$ and how the T^* line evolves with increasing doping level in the overdoped regime.

Emery and Kivelson [14] have emphasized the importance of phase fluctuations of the order parameter $\psi = |\psi|e^{i\theta}$ for HTS because of the two-dimensionality (2D), low superfluid density (n_s), and short coherent length (ξ). They argued that the value of T_c in the underdoped regime is determined primarily by the phase ordering. A sketch of the phase diagram of HTS as a function of temperature and doping level (p) proposed by EK model is shown in Fig. 1. T^{MF} is the mean-field transition temperature predicted by BCS-Eliashberg theory, and T_θ^{max} is the upper bound of the phase ordering temperature at which phase order would disappear. The characteristic energy scale for phase fluctuations is the zero-temperature “phase stiffness” $V_0 = \hbar^2 n_s(0) a / 4m^*$, and T_θ^{max} is proportional to V_0 . In the underdoped and optimally doped regime, due to small superfluid density and therefore small phase stiffness, the strong phase fluctuations cause the T_θ^{max} to fall below T^{MF} , i.e., $T_\theta^{\text{max}} < T^{\text{MF}}$. Therefore, the actual value of T_c is determined by T_θ^{max} . This model can explain the proportion of T_c with the doping level and regards the pseudogap as the effect of preformed Cooper pairs in

this regime. In the overdoped regime, T_θ^{max} is higher than T^{MF} , and the actual value of T_c is determined by T^{MF} .

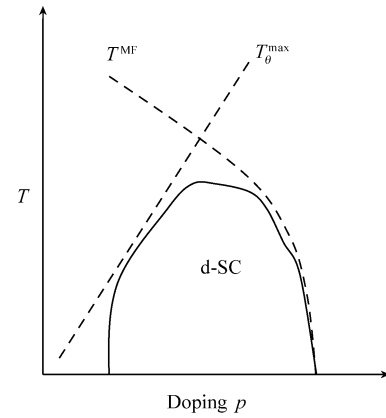


Fig. 1 A sketch of the phase diagram of high-temperature superconductors [14].

From the EK model, there should exist some dynamic Cooper pairs, namely some evidences of superconductivity above T_c . More and more experimental evidences supporting this model have been reported. Corson *et al.* [19] detected dynamic vortices by high-frequency ac conductivity and found that there exist dynamic vortices in a temperature range above T_{c0} in underdoped Bi-2212. Xu *et al.* [20] have surprisingly found that the Nernst signals due to vortex-like excitations still persist in the pseudogap region above T_c . Recently Wang *et al.* [21] detected finite diamagnetization signal above the transition temperature T_c by torque magnetometry. These experiments strongly support the first category of the theoretic models in which the T_c value in underdoped regime is determined by the loss of phase coherence.

In this paper, we first introduce the concepts of Nernst effect and explain our notation. Then, an overview of Nernst results on hole-doped HTS is given, and the discussion relevant to theoretic models is followed. Finally, we summarize the results and conclusions.

2 Vortex Nernst effect

A general definition of the Nernst effect is the appearance of a transverse electric field E_y in response to a temperature gradient ∇T in the x -axis direction, in the presence of a perpendicular magnetic H in the z -axis direction, and under open circuit conditions. Figure 2 (a) is a sketch of the quasiparticle Nernst effect in normal metals. The Nernst coefficient ν is defined as:

$$\nu = \frac{E_y}{|\partial_x T| B_z} \quad (1)$$

The Nernst signal is defined as $e_y(H, T) = E_y / |\nabla T|$.

Because of a so-called “Sondheimer cancellation” [22] the Nernst effect is usually small in normal metals or in the

normal state of superconductors where transport by quasi-particles is dominant. In the presence of a longitudinal temperature gradient ($-\nabla T$) and perpendicular magnetic field (\mathbf{H}), the total electrical current density in a metal is:

$$\mathbf{j} = \sigma \cdot \mathbf{E} + \alpha \cdot (-\nabla T) \quad (2)$$

Where σ is the 2D electrical conductivity tensor and α is the 2D Peltier conductivity tensor. The current density in x and y direction are j_x and j_y , respectively. To satisfied the boundary condition, we get $j_x = 0$ and $j_y = 0$, i.e.,

$$j_x = \sigma E_x - \sigma_H E_y + \alpha (-\partial_x T) = 0 \quad (3a)$$

$$j_y = \sigma_H E_x + \sigma E_y + \alpha_{yx} (-\partial_x T) = 0 \quad (3b)$$

In Eq. (3a), if we ignore the small term $\sigma_H E_y$, we get the Seebeck coefficient $S = \frac{E_x}{-\partial_x T} = \frac{\alpha}{\sigma}$. Using the Hall angle $\tan \theta = \sigma_{xy} / \sigma$ in Eq. (3b), finally we can obtain:

$$\mathbf{v} = \frac{E_y}{(-\partial_x T)B} = \left(\frac{\alpha_{xy}}{\sigma} - S \tan \theta \right) \frac{1}{B} \quad (4)$$

The value of these two terms in Eq. (4) [also shown in Fig. 2 (a)] are comparable but in opposite direction. So the Nernst signal in normal metals and normal state of type II superconductors is very small and scales linearly with applied magnetic field H . This is called ‘‘Sondheimer cancellation’’ [22]. Sondheimer has already proved about 60 years before that, if the Hall angle is independent of energy, these two terms can be cancelled completely. In the normal state of HTS, ν is about 10^{-8} V/kT while $(S \tan \theta)/B$ is $10^{-6} - 10^{-7}$ V/kT, it can be seen that the cancellation in HTS is quite complete [20].

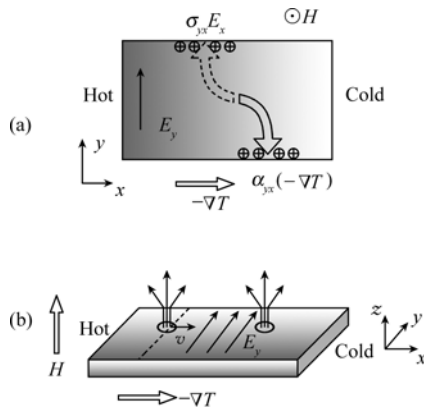


Fig. 2 The concept of Nernst effect for normal quasiparticles (a) and vortices (b). In (a) the Hall current flow ($\sigma_{yx}E_x$) and the off-diagonal Peltier current flow [$\alpha_{yx}(-\nabla T)$] cancel each other; In (b) the vortex Nernst signal in the vortex-liquid state of type II superconductors is the leading response because of the peculiar symmetry expressed in the equation $\mathbf{E} = \mathbf{B} \times \mathbf{v}$.

It is well known that in type II superconductors, there exists a mixed state when the applied magnetic field is between the lower critical magnetic field H_{c1} and upper critical magnetic field H_{c2} . The external magnetic field penetrates

the superconductor inhomogeneously as magnetic vortices (each carrying a flux quantum $\Phi_0 = h/2e$). Therefore, for a type-II superconductor (in the vortex-liquid state), a new set of excitations—vortices—are driven by temperature gradient $\nabla T \parallel x$. Vortices diffuse down the gradient with velocity v . As each vortex core cross the line between a pair of transverse voltage electrodes, the 2π phase slip of the condensate phase leads to a Josephson electric field given by $\mathbf{E} = \mathbf{B} \times \mathbf{v}$, which is called vortex Nernst effect. The concept of vortex Nernst effect is sketched in Fig. 2 (b). The vortex Nernst signal in the vortex-liquid state is much larger than the quasiparticle Nernst signal in normal state. Therefore, Nernst signal is regarded as a very sensitive probe of vortex excitations.

The samples used in Nernst effect measurement are usually cut into rectangular shape. A small thin-film heater with a size of 0.5×0.5 mm² in area was closely attached to the end of the sample to produce a small temperature gradient (typically 5 K/cm) along the longitudinal direction (x -direction), and the magnetic field was applied along the z -direction (the c -axis of the sample). Thus, the Nernst electric field is along the y -direction, which was measured by a Keithley nanovoltmeter. The temperature gradient is measured by two small Cernox thermometers (CX-1050-BR from Lake Shore Cryotronics) thermally anchored to the two ends of the sample. At fixed temperatures the Nernst signal was recorded while the magnetic field was sweeping slowly. The temperature was regulated by a Lakeshore temperature controller and the temperature drift was less than 5 mK during the measurement. The magnetic field is swept in both positive and negative directions, and only the field-asymmetric part of the voltage signal is taken as the Nernst signal.

3 Vortex Nernst signals above T_c in hole doped HTS

The first experimental evidence of vortex Nernst signals above T_c in $\text{La}_{2-x}\text{Sr}_x\text{CuO}_4$ (LSCO) system (x from 0.05 to 0.17) was reported by Xu *et al.*[20]. They surprisingly found that the vortex Nernst signals in underdoped LSCO persist in a temperature range of 50–100 K well above T_c . Figure 3 shows the traces of the Nernst signal ($E_y/|\nabla T|$) versus the applied magnetic field H of a LSCO sample ($x=0.10$, $T_{c0} = 28$ K), taken at fixed temperatures. At temperatures well below T_{c0} , all the curves have the characteristic features of the vortex Nernst effect: the signal e_y remains zero in the solid vortex lattice state where all the vortices are pinned; after a first order vortex solid to liquid phase transition at H_m , the motion of a large number of vortices leads to a sharp increase of e_y ; it tends to reach a maximum at a higher characteristic field scale H^* (H^* is beyond the maximum of the applied magnetic field in some low temperatures). With increasing temperatures, H_m tends to smaller values and disappears as T is close to T_{c0} . As T is above T_{c0} , the Nernst signal is still a sizeable fraction of low- T values. At higher T , the signal decreases gradually, approaching a straight line of

negative slope, which we identify with the background signal $v_n B$ from the normal charge carriers (holes). Other LSCO samples exhibit similar traces of e_y versus H . The temperature dependence of Nernst coefficient v , calculated from the initial slope of e_y versus H curves, is shown in the inset of Fig. 3. With decreasing temperatures, v deviates from the high-temperature background and increases quickly at the onset temperature T_v , then reaches a maximum below T_c , and finally decreases to zero as the vortex becomes pinned. In the temperature range between T_{c0} and T_v there exists anomalously large Nernst signal, which has been interpreted as evidence for strong superconducting phase fluctuations in

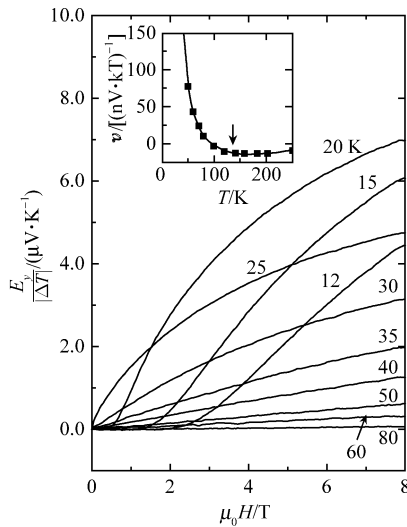


Fig. 3 The H dependence of Nernst signal for a typical underdoped LSCO sample ($x = 0.10$, $T_{c0} = 28$ K). Inset: the temperature dependence of Nernst coefficient v for this sample. The arrow indicates the position where v increases abruptly, i.e., the onset temperature (T_v) of anomalous vortex Nernst signal.

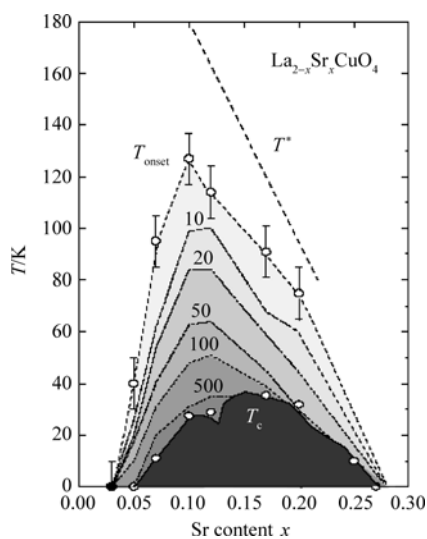


Fig. 4 The phase diagram of LSCO showing the Nernst region between T_c and T_{onset} . The numbers on the contour curves indicate the value of the Nernst coefficient v in $\mu\text{V}/\text{K}$. The dashed line is T^* estimated from heat capacity measurements.

this region. In the conventional superconductors, as the temperatures exceed T_c , the vortices vanish immediately, so the vortex Nernst signal should be immersed into the background signal due to normal charge carriers. The temperature at which the vortex-like excitations disappear is defined as a new characteristic temperature T_v . T_v in the underdoped regime is much higher than T_c but lower than T^* where the pseudogap opening is.

A phase diagram illustrated by the contour plot of the vortex Nernst signals for LSCO system is shown in Fig. 4. It can be seen that T_v (denoted as T_{onset} in Fig. 4) is generally lower than T^* in underdoped HTS, but it scales with T^* in a large doping level. This result strongly indicates that the vortex-like excitations persist in the pseudogap regime, which implies that the transition at T_{c0} is driven by the loss of long-range phase coherence. Some aspects of superconductivity may reveal themselves at temperatures much higher than T_c .

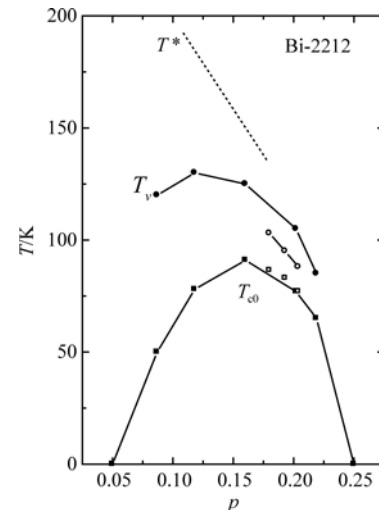


Fig. 5 The phase diagram of Bi-2212 showing the Nernst region between T_v and T_{c0} . The data represented by solid squares and circles are taken from Ref. [27] and the data represented by the open symbols are taken from Ref. [28].

The large anomalous Nernst signals caused by the vortex-like excitations in the pseudogap state have been observed in a variety of hole-doped superconducting cuprates, including LSCO [20, 23], YBCO [24–25], Bi-2201 [23] and Bi-2212 [24, 26]. All of the Nernst studies on the hole-doped HTS systems exhibit similar results. For example, Figure 5 shows the phase diagram as T_v and T_{c0} versus doping level (p) for Bi2212. The data are taken from Refs. [27] and [28]. All the Nernst results establish that it is a common feature for hole-doped HTS that there exist vortex-like excitations in a certain temperature range ($T_{c0} < T < T_v$) above T_{c0} , which strongly implies that T_{c0} is primarily determined by the loss of phase coherence due to spontaneous vortex-antivortex unbinding in $H=0$. Although the Nernst region does not extend all the way to the pseudogap temperature T^* , the Nernst results still provide strong evidences supporting the theoretic

models (such as EK model) in which the pseudogap state is a precursor to the d-wave superconductivity. (The Nernst results in the electron-doped cuprates are quite different to those in the hole-doped cuprates, see Refs. [26, 29]).

It can be seen clearly in Fig. 5 that none of the T^* and T_v lines drops to zero near the proposed quantum critical point (QCP) as p increases across the proposed quantum critical point (QCP) at $p \sim 0.19$ [18] and T_v line remains below T^* line in overdoped regime. This implies that the Nernst results are inconsistent with the 3rd category of the theoretic models introduced in Section 1. Furthermore, T_v is still below T^* in overdoped HTS, which does not support the recent theoretic proposal that the lines of T_v and T^* should cross near 0.19 [30].

The upper critical field H_{c2} is an important characteristic parameter that describes the mixed state to normal state transition. However, $H_{c2}(T)$ is a rather poorly established quantity compared with the other parameters of the superconducting state. Nernst effect measurement can provide a direct determination of $H_{c2}(T)$. When the applied magnetic field is larger than $H_{c2}(T)$, the superconducting state becomes a normal state and the vortex excitations should also disappear simultaneously. Thus the vortex Nernst signal $e_y(H)$ goes to zero as H approaches $H_{c2}(T)$. For a conventional type II superconductor, the $H_{c2}(T)$ line should terminate at T_{c0} . Wang *et al.* [31] extended the measurement of the Nernst effect to high magnetic field (up to 40 T) and determined the H_{c2} near T_{c0} by extrapolating the $e_y(H)$ curves to zero. They surprisingly found that the value of $H_{c2}(T)$ determined by the Nernst signal at high fields still remains an extraordinarily high value at T_{c0} for LSCO, which means the H_{c2} line does not terminate at T_{c0} . Figure 6 shows a contour plot of e_y in the T - H plane for a slightly overdoped LSCO sample. $H_{c2}(T)$ values estimated from the extrapolation of the $e_y(H)$ curves are shown as solid circles. It is clearly seen that $H_{c2}(T)$ line does not drop to zero as T increases across T_{c0} . This behavior is in sharp contrast with conventional type-II superconductors where $H_{c2}(T)$ decreases linearly to zero near T_c , i.e., $H_{c2} \propto (T_c - T)$.

Further investigation of Nernst experiments on Bi2201 shows again the similar H_{c2} behavior. Moreover, the $H_{c2}(T)$ is almost T -independent for a large temperature range [29]. The constancy of H_{c2} across T_c is apparently inconsistent with the mean-field BCS scenario in which the order parameter $|\psi|^2$ vanishes dramatically as $T > T_{c0}$. The fact that the depairing field $H_{c2}(T)$ remains finite for a significant interval above T_c means that $|\psi|$ remains finite even above T_c . This result strongly indicates that the collapse of the Meissner state at T_c is driven by the loss of long-range phase coherence. The loss of the phase coherence arises from the spontaneous generation of vortices. Actually the $|\psi|$ would go to zero at a much higher temperature (probably at T^* as suggested in some theoretic models) than T_c . The anomalous behavior of H_{c2} is consistent with the vortex interpretation of the Nernst signal above T_c .

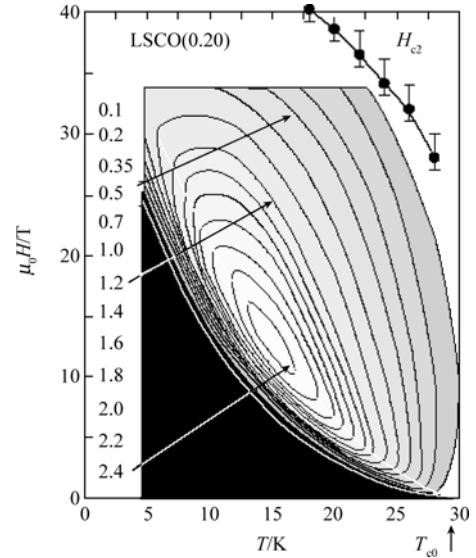


Fig. 6 The Nernst signal e_y represented as a contour plot in the T - H plane. Values of e_y (in $\mu\text{V/K}$) at successive contour lines are shown on the left column (white arrows). $H_{c2}(T)$ values estimated from the extrapolation of the $e_y(H)$ curves are shown as solid circles. The data are taken from Ref. [31].

Recently the Nernst effect for an underdoped ($x=0.09$) and an optimally doped ($x=0.15$) LSCO single crystals was measured as the magnetic field applied along the different directions [32]. The Nernst electric field is $E_y = \alpha |\nabla T| H \cos \theta$ when there is an angle θ between the applied magnetic field H and the c -axis direction of the sample. Generally speaking, the parameter α also depends on the angle θ (the angle between H and the c -axis). Only when the sample is isotropic or the vortex-like excitation is strictly two-dimensional, E_y is in proportion to $H \cos \theta$. However, when $H \parallel ab$ plane, the Nernst signal along the c -axis drops below the noise level quickly as $T > T_c$ for the underdoped sample. Moreover, the in-plane Nernst signals with field at different angles show a nice scaling behavior with the c -axis component of the field, i.e., $E_y \propto H \cos \theta$. It is well known that HTS is a system of strong anisotropy. This result strongly implies a 2D feature of the vortex-like excitations in the pseudogap region.

Up to now, the consensus about the vortex Nernst effect in the hole-doped HTS can be summarized as below.

(i) In the mixed state of hole-doped HTS, there exists a large vortex Nernst signal that does not disappear at superconducting transition temperature T_{c0} , and still persists to a certain temperature T_v above T_{c0} . T_v is usually lower than T^* .

(ii) From the Nernst signal versus H curves, the upper critical field H_{c2} can be deduced. This H_{c2} values are larger than those obtained from the usual method and show a weak dependence on T . Most surprisingly H_{c2} remains at extraordinarily high values as $T \rightarrow T_{c0}$.

(iii) The vortex-like excitations in the pseudogap state are strictly two-dimensional.

4 Discussions

Anomalous Nernst signals due to vortex-like excitations have been observed at temperatures well above T_{c0} in a variety of hole-doped HTS systems. According to the general phase diagram of HTS, as the doping concentration decreases from optimally-doping, T_c decreases, but T^* increases on the contrary in a certain doping range. The vortex-like excitation region above the “superconducting dome” cannot be understood in the frame of conventional superconducting fluctuations, which implies that the mechanism of HTS is substantially different from that of conventional superconductors. This discovery has inspired a revisit to the theory of superconducting fluctuations in the cuprates. Ussishkin *et al.* [33] suggest that Gaussian superconducting fluctuations above T_c are able to explain the Nernst effect for the optimally doped and overdoped regimes. But their model fits the Nernst signal poorly in the underdoped regime. The work of Carlson *et al.* [34] predicts that in the hole-doped cuprates the fluctuations in the phase of the order parameter would dominate the Nernst signal up to a certain temperature above T_c , and at still higher temperatures there should be contributions to the Nernst effect from fluctuations both in phase and the amplitude of the order parameter.

In the superconducting state, the pair condensate state described by the macroscopic wave function $\widehat{\Psi} = |\Psi| e^{i\theta}$ exhibits long-range phase coherence. In conventional superconductors, the pairing amplitude $|\Psi|$ vanishes above T_c , and T_c is determined by the mean-field BCS transition temperature T^{MF} . Fluctuations of the order parameter $\widehat{\Psi}$ are fluctuations of the amplitude $|\Psi|$. The Gaussian approximation provides a good description of fluctuation in conventional low- T_c superconductors. In low-dimensional and low-superfluidity-density systems like HTS, the phase fluctuations become important due to the low phase stiffness [14]. Therefore, it is not surprising that the Gaussian fluctuation description does not apply to HTS. Just after the discovery of HTS, Baskaran *et al.* [35] and Doniach and Inui [36] noted that T_c in underdoped HTS must be controlled by loss of phase coherence. Emery and Kivelson [14] further developed the phase-disordering scenario and proposed the sketch phase diagram as shown in Fig. 1. They suggested that the value of T_c in underdoped regime should be determined by the temperature scale for phase ordering, which is proportional to the superfluid density. The Uemura plot that T_c in underdoped HTS follows a universal, linear dependence on n_s/m^* , which is inferred from muon spin relaxation (μ SR) provide early evidence that T_c scales with the superfluid density, consistent with this scenario [37]. Corson *et al.* [19] measured the ac conductivity in two underdoped Bi-2212 thin films at THz frequencies and found that the kinetic inductance persistence to ~ 25 K above T_c . This result provides further evidence that there exist dynamics vortex excitations above T_c in HTS. The broad range of tempera-

tures above T_{c0} in which the vortex signal is observed by the highly sensitive Nernst effect experiment presents the most compelling evidence for the phase-disordering scenario.

The Kosterlitz-Thouless (KT) transition is a prototypical example of the phase-disordering transition [38–40]. Vortex-antivortex unbinding at the KT transition temperature T_{KT} destroys long-range phase coherence and superfluidity, but the pair amplitude $|\Psi|$ remains finite above T_{KT} . The phase disordering driven by the thermally generated vortices at T_c in HTS is the 3D analog of the KT transition in 2D system. According to the EK model, the pairing amplitude $|\psi|$ is no longer zero when the pseudogap opens as $T < T^*$, and the loss of the Meissner effect (flux-expulsion) in the temperature range $T_c < T < T^*$ corresponds to a loss of long-range phase coherence of Cooper pairs caused by the vortex excitations. As a self-consistent scenario, the depairing field H_{c2} should also remain at a large finite value at T_c , instead of approaching zero.

However, it should be noted that in HTS systems, the Nernst region ($T_c < T < T_v$) does not extend all the way to the pseudogap temperature T^* . As shown in Figs. 4 and 5, T_v lies between T_c and T^* . Recently, Curty and Beck [41] have proposed that there are two different regimes in the pseudogap state: one is near the superconducting state, phase correlations of Cooper pairs are important up to the temperature T_ϕ ; the other is above T_ϕ , the pseudogap region is only determined by the amplitudes, and phases are uncorrelated. Namely, the temperature regime between T_ϕ and T_c is characterized by the phase fluctuations (dynamical correlations) of Cooper pairs; as T is above T_ϕ , the pseudogap region is only determined by the amplitudes, and the phase correlation disappears completely. We suggest that the characteristic temperature T_v represents the temperature scale T_ϕ . Therefore, the Nernst experiment can directly determine the T_ϕ temperature scale, and it can be understood why the Nernst signal of vortex-like excitation does not extend all the way to T^* .

5 Summary

In the hole-doped HTS, a large regime above T_c in which an anomalous Nernst signals exist are uncovered by the Nernst experiments. The anomalous Nernst signals are interpreted as the evidence that there exist vortex-like excitations in a large temperature region above T_c . The depairing field H_{c2} determined by Nernst effect remains at a large finite value at T_c , instead of approaching zero. Therefore, the Nernst results presents the most compelling evidence for the phase-disordering scenario in which thermally generated vortices destroy long-range phase coherence at T_{c0} and the pseudogap state is a pre-formed pairing state. The vortex-like excitations in the pseudogap state are of 2D feature for both underdoped and optimally doped HTS.

As proposed by the theoretic works of Curty and Beck

[41], there are two different regimes in the pseudogap state: one is near the superconducting state, phase correlations of Cooper pairs are important up to the temperature T_v ; the other is between T^* and T_v , the pseudogap region is only determined by the amplitudes, and phases are completely uncorrelated.

Acknowledgements This work was partially supported by the National Natural Science Foundation of China (Grant No. 10225417) and the National Basic Research Program of China (Grant No. 2006CB601003).

References

1. Puchkov A.V., Fournier P., and Timusk T., *J. Phys:Condens. Matter*, 1996, 8: 10049–10082
2. Damascelli A., Hussain Z., and Shen Z. X., *Rev. Mod. Phys.*, 2003, 75: 473–542
3. Hewitt K. C. and Irwin J. C., *Phys. Rev. B.*, 2002, 66: 054516-1-9
4. Matsuda A., Sugita S., and Watanabe T., *Phys. Rev. B*, 1999, 60: 1377–1381
5. For a review, see Timusk T. and Statt B., *Rep Prog Phys* 1999, 62: 61–122
6. For a earlier review, see Batlogg B., Hwang H. Y., Takagi H., Cava R. J., Kao H. L., and Kwo J., *Physica C*, 1994, 235–240: 130–133
7. Gunnarsson O., Calandra M., and Han J. E., *Rev. Mod. Phys.*, 2003, 75: 1085–1099
8. Bucher B., Steiner P., Karpinski J., Kaldis E., and Wachter P., *Phys. Rev. Lett.*, 1993, 70: 2012–2015
9. Takagi H., Batlogg B., Kao H. L., Kwo J., Cava. R. J., Krajewski J. J., and Peck. W. F., Jr., *Phys. Rev. Lett.*, 1992, 69: 2975–2978
10. Ito T., Takenaka K., and Uchida S., *Phys. Rev. Lett.*, 1993, 70: 3995–3998
11. Watanab T., Fujii T., and Matsuda A., *Phys. Rev. Lett.*, 1997, 79: 2113–2116
12. Chien T. R., Wang Z. Z., and Ong N. P., *Phys. Rev. Lett* 1991, 67: 2088–2091
13. Matthey D., Gariglio S., Giovannini B., and Triscone J.-M., *Phys. Rev. B*, 2001, 64: 024513-1-5
14. Emery V. J. and Kivelson S. A., *Nature (London)*, 1995, 374: 434–437
15. Anderson P. W., *Science*, 1987, 235: 1196–1199
16. Nagaosa N. and Lee P. A., *Phys. Rev. B.*, 1992,45: 966–970
17. Tallon J. L., Williams G. V. M., Staines M. P., and Bernhard C., *Physica C*, 1994, 235–240: 1821–1822
18. Tallon J. L. and Loram J. W., *Physica C*, 2001, 349: 53–68
19. Corson J., Mallozzi R., Orenstein J., Eckstein J. N., and Bozovic I., *Nature (London)*, 1999, 398: 221–223
20. Xu Z. A., Ong N. P., Wang Y., Kakeshita T., and Uchida S., *Nature (London)*, 2000, 406: 486–488
21. Wang Y., Li L., Naughton M. J., Gu G. D., Uchid S., and Ong N. P., *Phys. Rev. Lett.*, 2005, 95: 247002
22. Ong N. P., Wang Yayu, Ono S., Ando Y., and Uchida S., *Ann. Phys. (Leipzig)*, 2004, 13: 9–14
23. Wang Yayu, Xu Z. A., Kakeshita T., Uchida S., Ono. S., Ando. Y., and Ong N. P., *Phys. Rev. B*, 2001, 64: 224519-1-10
24. Ong N. P., Wang Yayu, Ono S., Ando Y., and Uchida S., *Ann. Phys. (Leipzig)*, 2004, 13: 9–14
25. Xu Z. A., Shen J. Q., Zhao S. R., Zhang Y. J., and Ong C. K., *Phys. Rev. B*, 2005, 72: 144527-1-5
26. Wang. Y., Ono. S., Onose. Y., Gu G., Ando. Y., Tokura Y., Uchida S., and Ong N. P., *Science*, 2003, 299: 86–89
27. Wang Y., Ph. D thesis, Princeton University, 2003 (unpublished)
28. Shen J. Q., Ph. D thesis, Zhejiang University, 2006 (unpublished)
29. Wang Y., Lu L., and Ong N. P., *Phys. Rev. B*, 2005, 73: 024510-1-20
30. Lee P. A., Nagaosa N., and Wen X. G., *Rev. Mod. Phys.*, 2006, 78: 17–85
31. Wang Yayu, Ong N. P., Xu Z. A., Kakeshita T., Uchida S., Bonn D. A., Liang R., and Hardy W. N., *Phys. Rev. Lett.*, 2002, 88: 257003-1-4
32. Wen H. H., Liu Z. Y., Xu Z. A., Weng Z. Y., Zhou F., and Zhao Z. X., *Europhys. Lett.*, 2003, 63: 583–589
33. Ussishkin I., Sondhi S. L., and Huse D. A., *Phys. Rev. Lett.*, 2002, 89: 287001-1-4
34. Carlson E. W., Emery. V. J., Kivelson S. A., and Orgad D. , 2002, *cond-mat / 0206217*
35. Baskaran G., Zou Z., and Anderson P. W., *Solid State Commun.*, 1987, 63: 973–976
36. Doniach S. and Inui M., *Phys. Rev. B*, 1990, 41: 6668–6678
37. Uemura Y. J., Luke G. M., Sternlieb B. J., Brewer J. H., Carolan J. F., Hardy W. N., Kadono R., Kempton J. R., Kiefl R. F., Kreitzman S. R., Mulhern P., Riseman T. M., Williams D. Ll., Yang B. X., Uchida S., Takagi H., Gopalakrishnan J., Sleight A. W., Subramanian M. A., Chien, C. L. Cieplak M. Z., Xiao Gang, Lee V. Y., Statt, B. W. Stro-nach C. E., Kossler W. J., and Yu X. H., *Phys. Rev. Lett.*, 1989, 62: 2317–2320
38. Kosterlitz J. M. and Thouless D. J., *J. Phys. C*, 1973, 6: 1181–1203
39. Beaseley M. R., Mooij J. E., and Orlando T. P., *Phys. Rev. Lett.*, 1979, 42: 1165–1168
40. Doniach S. and Huberman B. A., *Phys. Rev. Lett.*, 1979, 42: 1169–1172
41. Curty P. and Beck H., *Phys. Rev. Lett.*, 2003, 91: 257002-1-4